Published in final edited form as:
*Nat Mater*. 2012 December ; 11(12): 1081–1085. doi:10.1038/nmat3461.

# New Autonomous Motors of Metal-Organic Framework (MOF) Powered by Reorganization of Self-Assembled Peptides at interfaces

**Yasuhiro Ikezoe**[a], **Gosuke Washino**[b], **Takashi Uemura**[b], **Susumu Kitagawa**[b,c], and **Hiroshi Matsui**[a,*]

[a]Department of Chemistry and Biochemistry, City University of New York – Hunter College, 695 Park Ave., New York, NY 10065 (USA)

[b]Department of Synthetic Chemistry and Biological Chemistry, Kyoto University, Katsura, Nishikyo-ku, 615-8510, Kyoto (Japan)

[c]Institute for Integrated Cell-Material Sciences (iCeMS), Kyoto University, Yoshida, Sakyo-ku, Kyoto 606-8501 (Japan)

## Abstract

There have developed a variety of microsystems that harness energy and convert it to mechanical motion. Here we developed new autonomous biochemical motors by integrating metal-organic framework (MOF) and self-assembling peptides. MOF is applied as an energy-storing cell that assembles peptides inside nanoscale pores of the coordination framework. The robust assembling nature of peptides enables reconfiguring their assemblies at the water-MOF interface, which is converted to fuel energy. Re-organization of hydrophobic peptides could create the large surface tension gradient around the MOF and it efficiently powers the translation motion of MOF. As a comparison, the velocity of normalized by volume for the DPA-MOF particle is faster and the kinetic energy per the unit mass of fuel is more than twice as large as the one for previous gel motor systems. This demonstration opens the new application of MOF and reconfigurable molecular self-assembly and it may evolve into the smart autonomous motor that mimic bacteria to swim and harvest target chemicals by integrating recognition units.

Various artificial cells that can storage molecules in organic and inorganic cages are designed to generate mechanical motion efficiently by dissipating chemical free energy through chemical reactions or reorganization of molecules. Typically this continuous non-equilibrium condition is created by altering chemical environment around the cells via release/uptake of molecules. In many artificial motor systems, surfactants in or surrounded around cells of oil droplets[1,2] and camphor,[3] play roles to fuel their motion by Marangoni effect[4] where the release of molecules develops the anisotropic surface tension gradient around the cells, and these cells are pushed to the direction from low to high surface tension. Previously, gels were also used as storages for organic molecule and the release of these molecules triggered the motion by Marangoni effect.[5] However, organic molecules are only discharged in random directions, which is not quite efficient for the energy transfer. Ideally, if the ordered structure of molecules are released and then re-assembled at the interface, it could transfer chemical energy more efficiently and generate more forceful motion. For example, the motion of camphor disks at the water-air interface is strongly dependent on the

*Correspondence and requests for materials should be addressed to H.M. (hmatsui@hunter.cuny.edu).

Supplementary Information is linked to the online version of the paper at http://www.nature.com/nmat/index.html

order of self-assembled alkyl molecules at the interface.[3] Therefore, the assembly of released molecules is important to fuel the motion effectively. Because contemporary cellular movement in *in vitro* models relies upon the assembly and dynamics of encapsulated protein matrixes,[6–9] it would be desirable to develop cells that have ability to store molecules in highly ordered alignment and release them to the cell-water interface in well-organized structure for the development of more efficient but simpler hybrid host-guest systems.

To overcome these issues, we developed a new hybrid biomimetic motor system consisting of metal-organic framework (MOF) and diphenylalanine (DPA) peptide. The MOF, comprised of metal ions and bridging organic ligands, has recently emerged as an important family of nanoscale porous materials because of their unique structural and functional properties.[10–18] In this work, MOF is selected for the peptide storage because of its function to assemble small molecules in highly ordered pore array of coordination framework and to release guest molecules in more isotropic direction *via* bond-breaking of framework as compared to existing porous systems.[19] MOFs are also advantageous as vehicles of autonomous motors for their abilities to flexibly design rigidity, density, crystalline pore organization, and pore size so that the ideal combination of metal ions and ligands of MOFs can be selected with optimal light weight for the swimming motion and desired structure to release and reorganize guest peptides for controlling motion of MOF on air-liquid interfaces. The robust self-assembling nature of peptide[20–27] is also appropriate as a guest molecule to power the MOF motor because the released peptides from the MOF are re-self-assembled at the MOF-water interface in the highly-ordered structure is expected to generate the large surface tension gradient favoring strong Marangoni effect[5] and strong motor motion toward the higher surface tension side around the MOF. This novel driving mechanism of the peptide-incorporating MOF motion on the water surface consists of two steps: The first step is to release DPA peptides from the MOF by mixing ethylenediaminetetraacetic acid (EDTA) with the system. The partial destruction of MOF by EDTA allows releasing DPAs slowly through the ordered pores of MOFs. The second step is to accumulate and self-assemble DPAs at the water-MOF interface and to create large surface tension difference around the MOF, which can fuel the swimming motion since the released DPA assembly on the MOF creates the hydrophobic domain. Then the MOF motor moves toward the direction of the higher surface tension side. This peptide-MOF system is advantageous as compared with other artificial motor microsystems to accomplish the development of more efficient artificial motor system with faster movement and longer mobility lifetime because MOF can load the peptide fuels with much higher density in the highly ordered porous framework.[28,29] Another advantage of the use of porous MOF as peptide storage is its highly organized pore geometry, where the released DPA peptides can be robustly self-assembled at the MOF-water interface as these well-aligned guest peptides are released slowly from the MOF. In nature, the biological motors convert chemical free energy to mechanical power directly by creating isothermal and non-equilibrium conditions with biochemical reactions.[5,30,31] To keep away from equilibrium, cells wisely modify the environment by metabolizing resources and producing products and waste and simultaneously the system somehow exploits new resources as well as prevents the inhibitory effects of waste products.[1] This DPA peptide-incorporating MOF motor also creates the non-equilibrium condition by releasing peptides and transfer this chemical change to the energy of motor generated by the reconfiguration of DPA peptide self-assembly, which resembles to metabolizing and producing resources in nature. This type of technology could be applied to develop miniaturized robotic systems that sense the target chemicals, move toward the target location, and store them inside the porous frameworks. The outcome from this work may also shed light on the fundamental mechanisms of biological motors and chemotaxis in natural systems.

The structure of the hybrid MOF motor system is shown in Figure 1-(a). The MOF we used in this study is $[Cu_2L_2ted]_n$ where L is 1,4-benzenedicarboxylate with the pore size of 0.75 nm.[32,33] To incorporate DPA peptides in the MOF, the MOF particles are incubated in DPA peptides in 1,1,1,3,3,3-hexafluoro-2-propanol, which is a good solvent to dissolve DPA, and then immediately solvent is removed under a reduced pressure by a rotary pump. The incorporation of DPA in the MOF was confirmed by X-ray powder diffraction (XRPD), $N_2$ absorption, and particle size distribution measurements (supplementary information S-1, S-2, and S-3). Because the MOF decomposes in EDTA solution due to the removal of copper ions from the molecular framework, EDTA is used to trigger the release of DPA peptides from the MOF.[34,35] To compare the temporal dependence of velocity among neat MOF, neat DPA peptide, and DPA-MOF particles loading DPA peptides in the 20 % weight ratio to the MOF, each particle was dropped onto the surface of an aqueous solution containing EDTA (1 mM EDTA and 2 mM NaOH) and the motion was recorded as a movie by a light microscope. Then, the ImageJ software enables the quantification of the velocity change from the movie. The neat MOF particle is descended immediately to the bottom of the EDTA solution with no transitional and rotational motions and it does not decompose under the microscope in the time frame of this experimental setting. (◆ in Figure 1-(b), also see a movie in supplementary information S-4) This observation indicates that the rigidness of the selected MOF is high enough to avoid the rapid distraction under this condition after mixing with EDTA. The DPA peptide particles in the same size also show no movement in the same solution and small pieces are spread quickly on the water surface (× in Figure 1-(b) and also see a movie in supplementary information S-5). Actually the neat DPA peptide particles are instantaneously spread on the water surface and create the spike of velocity peak at 0–1s as they touches down on the aqueous surface. However, when the hybrid DPA-MOF particle is dropped onto the EDTA solution, it shows vigorous motion on the surface for more than 5 minutes (○ in Figure 1-(b) and also see a movie in supplementary information S-6). This DPA-MOF particle moved around on the surface at the maximum speed of 35 mm/s along the arrow in the image. The maximum velocity per volume (1 $mm^3$) of the motor system is calculated as 67 mm/s as the average diameter of DPA-MOF spherical particle is measured as 1 mm. The direction of motion is determined by an initial impulsion of DPA emission on the MOF, and after the direction of surface tension gradient is stabilized quickly the MOF particles move along the direction of gradient. This mechanism is similar to the droplet motion along the concentration gradient of reactive agents,[36] and this hypothesis is supported by the observation of constant unidirectional motion of DPA-MOF particles in the movie in supplementary information S-6. The translational motion for one of the fastest gel motor systems with the volume of 25 $mm^3$ is 50 mm/s,[5] where 90% of the gel body is filled with the liquid fuel. On the basis of this comparison, the velocity of normalized by volume for the DPA-MOF particle is 30 times faster and the kinetic energy per unit mass of fuel is 3 μJ/g, more than twice as large as the one for the hydrogel systems. Therefore, the DPA-MOF system can be realized to have remarkably efficient fuel conversion as an autonomous motor. Since the neat DPA particle does not move in the solution, the motion of the DPA-MOF particle must be powered by the release of DPA from the MOF. Actually after the DPA-MOF particles are moved for several minutes, dark thin layers of released DPA became visible at the water surface. Since once Cu ions are extracted from MOF by EDTA they are chelated as $[Cu(EDTA)]^{2-}$ rather than forming CuO and these complexes including ligand residues from MOF fragments are all soluble in aqueous solution.[34,35] Therefore, the dark aggregates at the interface are the reorganized DPA peptide assemblies with high density, supporting the hypothesis. (supplementary Information S-7). It should be noted that the extent of MOF decomposition has no effect in the velocity of MOF. Since there observes no correlation between concentration of EDTA in aqueous solution and velocity of MOF (supplementary Information Figure S-8), the released amount of peptide guest is not influenced sensitively by the extent of dissolution of MOF. Thus, this observation suggests that once the exiting

path of DPA is created by partial dissolution of MOF at the interface, DPA is emitted slowly and continuously in a constant rate from inside pores of MOF.

The mechanism of the motion of MOF particle is illustrated in Figure 2. As the surface of MOF is partially decomposed by EDTA, DPA peptides are released from well-ordered MOF pores (Figure 2-(a)). Since DPA peptides are emitted in the highly ordered assembling stream, the peptides are quickly re-assembled to form crystalline domains at the water-MOF interface and these self-assembled hydrophobic peptide domains decrease the surface tension on the side of MOF where more DPA peptides are released (Figure 2-(b)). Due to the surface tension difference, MOF particles are moved toward the direction of higher surface tension. It should be noted that when hydrophobic molecules with no robust self-assembling capability such as phenol and phenylalanine are incorporated in the MOF and injected to the EDTA solution, the motion is stopped immediately (supplementary Information S-9), which supporting the hypothesis that the re-assembly of released guest molecules in highly ordered structure at the interface is critical to fuel the continuous and strong motor motion of MOF (see a movie in supplementary Information S-10). To directly probe the degree of reorganization of DPA peptides after the release from MOF, the air-liquid interface is imaged with Brewster Angle Microscopy (BAM) while a peptide-MOF particle is moving on the interface. At 4 min after launching the particle to the interface, an increased number of bright domains evolve on the interface (Figure S-11-(a)). This increase in contrast reflects changes of indices of refraction at the air–water interface induced by the reorganization of crystalline peptides on the interface.[37] Thus, DPA peptides released from the MOF organize into assembled structures with the higher refractive index. When hydrophobic molecules with no robust self-assembling capability such as phenol and phenylalanine are incorporated in the MOF and injected to the EDTA solution, released phenol and phenylalanine show no molecular organization on the interfaces in BAM (Figures S-11-(b), (c)). Since the DPA-MOF system drives the motion and the phenol- and phenylalanine-MOFs create no motion after launching onto the EDTA solution, reorganization of guests at the interface is the major driving force to induce the autonomous swimming motion. In addition, to further strengthen the hypothesis about the role of crystalline pore structure of host in the reorganization of released DPA peptides on the air-liquid interface, we performed another control experiment; when neat DPA was dropped onto EDTA solution, there is no organized assembly of DPA on the air-liquid interface (Figure S-11-(d)), indicating that well-defined crystalline pore structure of MOF assists the reorganization of DPAs at the interface after released from MOF. Previously, there reported similar examples that polymers originally polymerized in MOFs were reassembled into unusual ordered structures with unique physical properties after frameworks were removed as compared to the ones polymerized without porous frameworks due to the influence of crystalline pore arrangement of MOFs.[38,39] In another control experiment, when DPA is incubated in a MOF with the smaller pore size ($[Cu_2L_2ted]_n$ where L is 1,4-naphthalenedicarboxylate with pore size of 0.57 nm) that is too small to accommodate DPA peptides inside (Supplementary Information S-3), there observed no mobility indicating that DPA is necessary to be incorporated in the framework for the generation of motor activity (supplementary Information S-9).

When DPA peptides released onto the water interface are collected on TEM grids, TEM image and electron diffraction pattern show that the DPA peptides are assembled into single crystalline structure (Figure 3-(a)).[40] Since salts and ligand residues from MOF fragments are washed out before imaging, these crystals are assembled from DPA nanocrystals. This result is consistent with the swimming mechanism that the generation of DPA crystals at the interface creates the surface tension gradient effectively for the motor activity. Here it is interesting that the shape of resulting DPA crystals to be in the planar parallelogram shape rather than typical tubular form.[21,41,42] Difference in crystallization environment on

different assembling substrates leads to polymorph nature of crystal forms of peptides with different nucleation pathways.[43] Since nucleation of DPA peptides occurs on the 2D air-liquid surface after releasing from the MOF, DPA crystals tend to be self-assembled in the planer form rather than cylindrical form. In addition, because molecules in MOF can be in extraordinary high density with unusual conformations in the pores,[38] it is plausible that these factors may influence the crystallization of DPA in unconventional way. It should also be noted that observing a crystalline domain of reorganized DPAs on the interface as small as 0.5 μm in diameter in TEM (Figure 3-(a)) is consistent with appearance of small and bright spot domains in BAM (Figure S-11-(a)).

Another control experiment was examined to verify the proposed mechanism of the movement with the surface tension difference created by the release of DPA peptides. If this convection of MOF particle is indeed driven by the Marangoni effect *via* the large surface tension gradient, the dispersion of self-assembled DPA peptides at the tail of MOF with 1,1,1,3,3,3-hexafluoro-2-propanol (HFP) should remove the lower surface tension domain. Thus, if the hexafluoropropanol is injected onto the aqueous surface when the MOF is in motion, the injection of the good solvent should freeze the motion immediately. This is exactly what was observed in Figure 3-(b). As hexafluoropropanol is injected at 42 s, the velocity of MOF is instantaneously dropped from 35 mm/s to 0 mm/s. (see also a movie in supplementary information S-12). Therefore, this observation further support the hypothesis that the released DPA peptides at the side of MOF generate the surface tension difference around the MOF motor and it powers the motion of MOF toward to the higher surface tension side. It should be noted that DPA also becomes soluble in aqueous solution at pH 10 and above this pH range the velocity of MOF is also dropped due to elimination of DPA re-assembly at the interface (supplementary information S-13).

Since the loaded DPA peptides are considered as fuels, the MOFs with more loaded DPAs should run in longer timeframe. To confirm this expected behavior, we examined the DPA-load dependence of the lifetime of motor motion with different loading amount of DPA in the 10, 20, and 30% weight ratios to the MOF. When DPA-loaded MOF particles in the diameter of 1 mm are dropped on the aqueous solution containing EDTA, the duration of MOF movement for 10, 20, and 30% with DPA-loading is approximately 300, 600, and 900 seconds, respectively, as shown in Figure 3-(c). This observation is consistent with our hypothesis that the lifetime of the MOF motion becomes longer as the loaded amount of DPA peptide fuels is increased. Interestingly, the velocity of MOF motion does not have any correlation with the load. This result indicates that the velocity is not dependent on the amount of loaded DPAs, and thus the degree and the rate of spatial inhomogeneity are more important driving forces for the MOF motor motion.

Because the release of DPA peptides from the MOF is probably not in the single direction, we may lose the efficient energy transfer from the self-assembly. To make the chemical motor motion more efficient, we created the vehicle, the MOF boat where samples in the diameter of 1 mm can fit inside the boat compartment and a very narrow slit at the tail allows the MOF motor to move into controlled direction (Figure 3-(d)). Because the slit makes the self-assembly of DPA peptides not only in anisotropic direction but also with higher density at single point, the MOF boat is expected to move faster in the anisotropic direction. Fig. 3-(e) is an overlaid optical image of the moving MOF boat (see a movie in supplementary information S-14). Comparing the motion of the neat DPA-MOF motor, the MOF boat with the same DPA loading amount moves faster even though total mass of the boat and MOF-DPA particle is heavier (Figure 3-(f)). Furthermore, the duration with the motion of MOF boat is also longer than the one for the neat DPA-MOF particle. This result indicates that the MOF boat could improve the energy transfer efficiency by properly designing the boat structure and controlling the surface tension distribution.

In conclusion, the hybrid biomolecular MOF assemblies incorporating the DPA peptides into the jungle-gym-like highly-ordered porous MOF structure, behave as autonomous biochemical motors as the DPA-MOF particles are dropped onto water solution containing EDTA. After MOF is partially decomposed at the interface, DPA is slowly released from the inside of MOF, which creates surface tension gradient triggering the autonomous motion. The freshly reorganized peptide crystalline domain is continuously generated at the interface as the slow release of DPA continues, enabling long-lasting motion with slow saturation of DPA on the interface. Eventually the surface tension gradient is dropped as the size of DPA domain dominants the hydrophilic area with the increased number of DPA crystals on the interface, and then the motion of MOF is slowed and eventually stopped after consuming all DPAs inside the MOF. It should be emphasized that the energy source of this generator is simply the free energy change of peptide emission, and it has similarity to biological motors, which also work through the dissipation of chemical energy. There are few artificial motor systems that have means to store the energy and release it by emitting hydrophobic peptides in highly re-assembled structure which triggers the mechanical motion via surface tension gradient. While this work demonstrates the creation of novel biomimetic artificial motor, this system may provide the better understanding of the mechanism of energy transduction and chemotaxis in biological systems with more depth of the study. The direction and the motion of MOF particles could be controlled by creating pH gradient or EDTA concentration gradient on liquid interfaces.[44] This type of artificial peptide-motor system could be developed into building blocks for targeted drug injection, osmotic pumping devices, and micro-actuators, and it may be further developed to smart machines with features that can change characteristically by sensing and adapting to new environments.[31]

## Methods

### Synthesis of MOFs and incorporation of DPA in the MOFs

MOFs used here were prepared according to previously reported methods.[32] In the case of 20% DPA incorporation in MOF, after 468 mg of DPA was dissolved in 1 ml of 1,1,1,3,3,3-hexafluoro-2-propanol, MOF, 2.34g, was added and then the solvent was extracted by rotary vacuum. The resulting solid DPA-MOF compound was further dried under the vacuum for 8 hours. For the 10% and 30 % DPA incorporation, 234 mg and 702 mg of DPA was dissolved in the same volume of 1,1,1,3,3,3-hexafluoro-2-propanol, respectively, and then they were mixed with 2.34g of MOF. The solvent was extracted by the same manner as descried above.

### Analysis of motion of hybrid DPA-MOF

For each experiment, a granular agglomerate of DPA-loaded MOF, neat DPA, or neat MOF with ca. 1 mm diameter was added on aqueous solution in 16 mL (or 200 μL) of 1 mM EDTA in NaOH (2 mM) in a transparent plastic petri dish (50 mm diameter and 7 mm depth or 8 mm diameter and 4 mm depth). The lateral motion on the liquid surface was monitored under irradiation of a halogen lamp from the bottom side through a light diffusing plate of a light microscope. The resulting movies were recorded as top-view video files at a frame rate of 24.39 frames per second. These sequential images are binarized to extract the particle motions, whose velocity change was analyzed by the image processing software, ImageJ, and its plugin, Mtrack2 (http://valelab.ucsf.edu/~nico/IJplugins/MTrack2.html).

### Instrumentation

For transmission electron microscopy (TEM), samples on the aqueous solution were directly transferred to a carbon-coated copper grid by dipping them at the interface. After the grid was washed by pure water, whose resistivity is 18.2 MΩ·cm, these samples were dried at room temperature. The samples were characterized by TEM (JEOL-JEM 2100) with an

acceleration voltage of 200 kV. X-ray powder diffraction (XRPD) data were collected on a Rigaku RINT 2000 Ultima diffractometer with Cu Kα radiation. The adsorption isotherms of $N_2$ at 77K were measured with a BELSORP-mini volumetric adsorption instrument using $N_2$ gas of high purity (99.9999%). Particle size distributions were measured by HORIBA Partica LA-950 laser diffraction particle size analyzer. Brewster angle micrographs (BAM) were taken with Accurion I-Elli2000 Imaging Ellipsometer.

## Supplementary Material

Refer to Web version on PubMed Central for supplementary material.

## Acknowledgments

All of works except chemical syntheses of MOFs were supported by the U.S. Department of Energy, Office of Basic Energy Sciences, Division of Materials Sciences and Engineering under Award No. DE-FG-02-01ER45935. Hunter College infrastructure is supported by the National Institutes of Health, the RCMI program (G12-RR003037-245476). Chemical syntheses of MOFs in Kyoto were supported by Grant-in-Aid for Scientific Research on Innovative Area “Emergence in Chemistry” from MEXT. H.M. acknowledges Japan Society for the Promotion of Science (JSPS) for supporting his collaboration in Kyoto University through Invitation Fellowship Program for Research in Japan. H.M was in the position of an Invited Professor at Institute for Integrated Cell-Material Sciences (iCeMS) during his sabbatical term in Kyoto University. Y.I. and H.M. thanks Prof. Raymond Tu (City College of New York) for the use and assistance of Brewster Angle microscopy.

## References

1. Hanczyc MM, Toyota T, Ikegami T, Packard N, Sugawara T. Fatty Acid Chemistry at the Oil-Water Interface: Self-Propelled Oil Droplets. J Am Chem Soc. 2007; 129:9386–9391. [PubMed: 17616129]
2. Sumino Y, Magome N, Hamada T, Yoshikawa K. Self-Running Droplet: Emergence of Regular Motion from Nonequilibrium Noise. Phys Rev Lett. 2005; 94:068301. [PubMed: 15783779]
3. Nakata S, Murakami M. Self-motion of a camphor disk on an aqueous phase depending on the alkyl chain length of sulfate surfactants. Langmuir. 2010; 26:2414–2417. [PubMed: 19877701]
4. Marangoni C. Ueber die Ausbreitung der Tropfen einer Flüssigkeit auf der Oberfläche einer anderen. Ann Phys. 1871; 219:337–354.
5. Gong JP, Matsumoto S, Uchida M, Isogai N, Osada Y. Motion of Polymer Gels by Spreading Organic Fluid on Water. J Phys Chem. 1996; 100:11092–11097.
6. Verkhovsky AB, Svitkina TM, Borisy GG. Self-polarization and directional motility of cytoplasm. Curr Biol. 1999; 9:11–20. [PubMed: 9889119]
7. Miyata H, Nishiyama S, Akashi K, Kinosita KJ. Protrusive growth from giant liposomes driven by actin polymerization. Proc Natl Acad Sci USA. 1999; 96:2048–2053. [PubMed: 10051592]
8. Upadhyaya A, van Oudenaarden A. Biomimetic systems for studying actin-based motility. Curr Biol. 2003; 13:R734–R744. [PubMed: 13678615]
9. Upadhyaya A, Chabot JR, Andreeva A, Samadani A, van Oudenaarden A. Probing polymerization forces by using actin-propelled lipid vesicles. Proc Natl Acad Sci USA. 2003; 100:4521–4526. [PubMed: 12657740]
10. Yaghi OM, et al. Reticular synthesis and the design of new materials. Nature. 2003; 423:705–714. [PubMed: 12802325]
11. Ferey G. Hybrid porous solids: past, present, future. Chem Soc Rev. 2008; 37:191–214. [PubMed: 18197340]
12. Bradshaw D, Claridge JB, Cussen EJ, Prior TJ, Rosseinsky MJ. Design, chirality, and flexibility in nanoporous molecular-based materials. Acc Chem Res. 2005; 38:273–282. [PubMed: 15835874]
13. Murray LJ, Dinca M, Long JR. Hydrogen storage in metal-organic frameworks. Chem Soc Rev. 2009; 38:1294–1314. [PubMed: 19384439]
14. Kitagawa S, Kitaura R, Noro S. Functional porous coordination polymers. Angew Chem Intl Ed. 2004; 43:2334–2375.

15. Li JR, Kuppler RJ, Zhou HC. Selective gas adsorption and separation in metal-organic frameworks. Chem Soc Rev. 2009; 38:1477–1504. [PubMed: 19384449]
16. Forster PM, Cheetham AK. Hybrid inorganic-organic solids: an emerging class of nanoporous catalysts. Top Catal. 2003; 24:79–86.
17. Lee J, et al. Metal-organic framework materials as catalysts. Chem Soc Rev. 2009; 38:1450–1459. [PubMed: 19384447]
18. Oh M, Mirkin CA. Chemically tailorable colloidal particles from infinite coordination polymers. Nature. 2005; 438:651–654. [PubMed: 16319888]
19. Uemura T, Yanai N, Kitagawa S. Polymerization reactions in porous coordination polymers. Chem Soc Rev. 2009; 38:1228–1236. [PubMed: 19384434]
20. Hartgerink JD, Beniash E, Stupp SI. Self-assembly and mineralization of peptide-amphiphile nanofibers. Science. 2001; 294:1684–1688. [PubMed: 11721046]
21. Reches M, Gazit E. Casting metal nanowires within discrete self-assembled peptide nanotubes. Science. 2003; 300:625–627. [PubMed: 12714741]
22. Bellomo EG, Wyrsta MD, Pakstis L, Pochan DJ, Deming TJ. Stimuli-responsive polypeptide vesicles by conformation-specific assembly. Nature Mater. 2004; 3:244–248. [PubMed: 15034560]
23. Pouget E, et al. Hierarchical architectures by synergy between dynamical template self-assembly and biomineralization. Nature Mater. 2007; 6:434–439. [PubMed: 17515916]
24. Ura Y, Beierle JM, Leman LJ, Orgel LE, Ghadiri MR. Self-Assembling Sequence-Adaptive Peptide Nucleic Acids. Science. 2009; 325:73–77. [PubMed: 19520909]
25. Banwell EF, et al. Rational design and application of responsive alpha-helical peptide hydrogels. Nature Mater. 2009; 8:596–600. [PubMed: 19543314]
26. Mershin A, Cook B, Kaiser L, Zhang SG. A classic assembly of nanobiomaterials. Nature Biotech. 2005; 23:1379–1380.
27. Williams RJ, et al. Enzyme-assisted self-assembly under thermodynamic control. Nature Nanotech. 2009; 4:19–24.
28. McKinlay AC, et al. BioMOFs: Metal-Organic Frameworks for Biological and Medical Applications. Angew Chem Intl Ed. 2009; 49:6260–6266.
29. Rabone J, et al. An Adaptable Peptide-Based Porous Material. Science. 2010; 329:1053–1057. [PubMed: 20798314]
30. Mitsumata T, Ikeda K, Gong JP, Osada Y. Solvent-driven chemical motor. Appl Phys Lett. 1998; 73:2366–2368.
31. Nakata S, Murakami M. Self-motion of a camphor disk on an aqueous phase depending on the alkyp chain length of sulfate surfactants. Langmuir. 2009; 26:2414–2417. [PubMed: 19877701]
32. Seki K, Mori W. Synthesis and characterization of microporous coordination polymers with open frameworks. J Phys Chem B. 2002; 106:1380–1385.
33. Uemura T, et al. Unveiling thermal transitions of polymers in subnanometre pores. Nature Communications. 2010; 1:83–91.
34. Uemura T, Ono Y, Kitagawa K, Kitagawa S. Radical polymerization of vinyl monomers in porous coordination polymers: Nanochannel size effects on reactivity, molecular weight, and stereostructure. Macromolecules. 2008; 41:87–94.
35. Uemura T, Ono Y, Hijikata Y, Kitagawa S. Functionalization of coordination nanochannels for controlling tacticity in radical vinyl polymerization. J Am Chem Soc. 2010; 132:4917–4924. [PubMed: 20225869]
36. Dos Santos FD, Ondarçuhu T. Free-Running Droplets. Phys Rev Lett. 1995; 75:2972–2975. [PubMed: 10059456]
37. Lheveder C, et al. A new Brewster angle microscope. Rev Sci Instrum. 1998; 69:1446–1450.
38. Yanai N, et al. Fabrication of Two-Dimensional Polymer Arrays: Template Synthesis of Polypyrrole between Redox-Active Coordination Nanoslits. Angew Chem Intl Ed. 2008; 47:9883–9886.
39. Uemura T, et al. Highly Photoconducting pi-Stacked Polymer Accommodated in Coordination Nanochannels. J Am Chem Soc. 2012; 134:8360–8363. [PubMed: 22574905]

40. Reches M, Gazit E. Controlled patterning of aligned self-assembled peptide nanotubes. Nature Nanotech. 2006; 1:195–200.

41. Görbitz CH. Nanotube formation by hydrophobic dipeptides. Chem Eur J. 2001; 7:5153–5159. [PubMed: 11775688]

42. Görbitz CH. The structure of nanotubes formed by diphenylalanine, the core recognition motif of Alzheimer's beta-amyloid polypeptide. Chem Commun. 2006:2332–2334.

43. Wolde, PRt; Frenkel, D. Enhancement of Protein Crystal Nucleation by Critical Density Fluctuations. Science. 1997; 277:1975–1978. [PubMed: 9302288]

44. Lagzi I, Soh S, Wesson PJ, Browne KP, Grzybowski B. a Maze solving by chemotactic droplets. J Am Chem Soc. 2010; 132:1198–1199. [PubMed: 20063877]

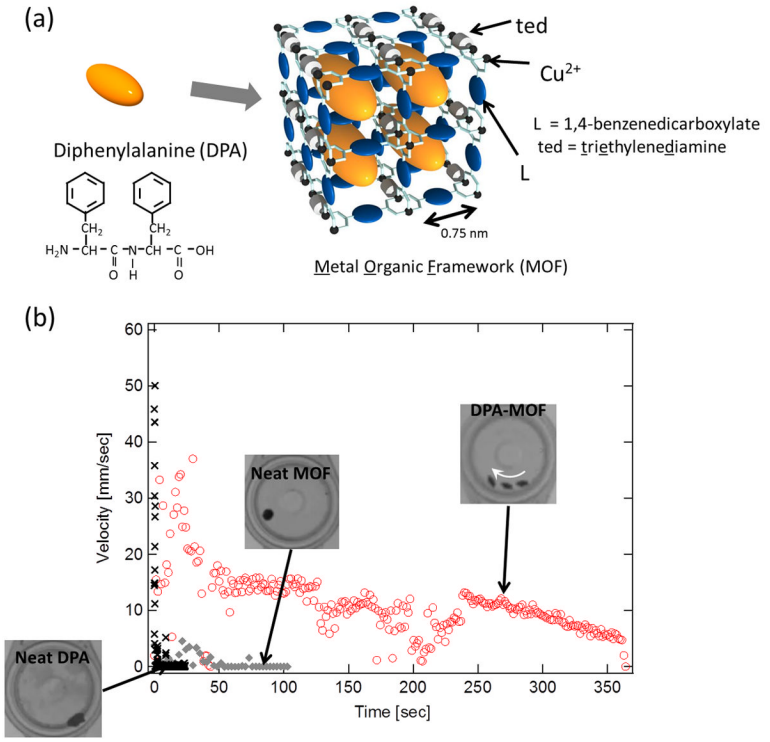


**Figure 1.**

Hybrid peptide-MOF motor. (a) Structures of host MOF and guest DPA peptide. (b) Velocity changes of DPA-MOF, neat MOF, and neat DPA with time in an aqueous solution containing 1 mM EDTA and 2 mM NaOH. Insets show overlaid optical image of the DPA-MOF, neat MOF, and neat DPA. Only DPA-MOF moves in this experimental condition and the motion is shown by a white arrow.

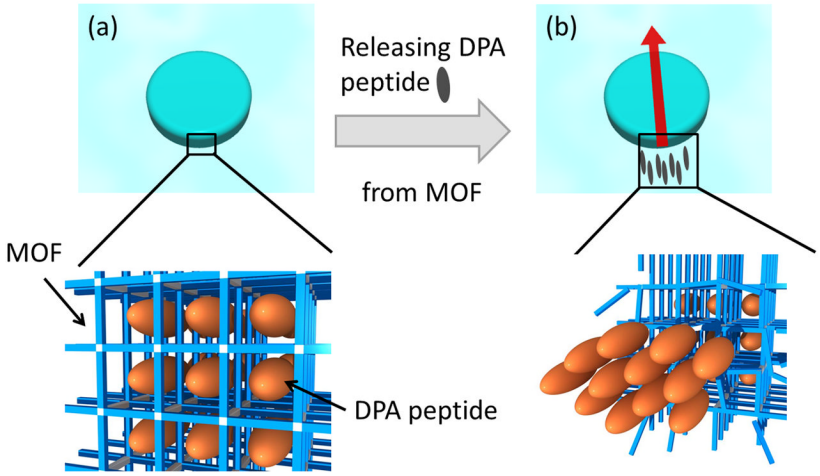


**Figure 2.**
Illustration of mechanism of DPA-MOF motion. (a) before releasing DPA peptides, MOF incorporates DPA peptides on the well-ordered alignment in nanoscale pores, (b) after releasing DPA peptides, the re-assembly of DPA peptides form the hydrophobic domain at the end of MOF particle. Since this domain lowers the surface tension of MOF on the released side, MOF particle moves with surface tension gradient via Marangoni effect.

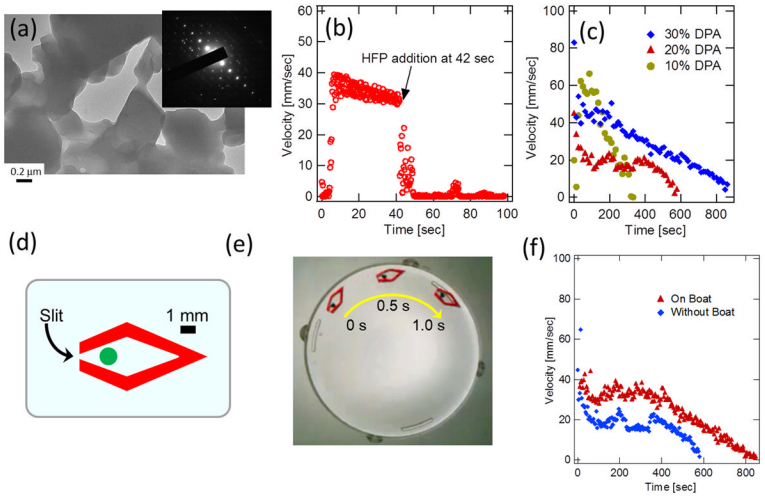


**Figure 3.**

DPA-MOF motor powered by self-assembly of DPA peptides at interface. (a) TEM image of released DPA peptides at the MOF-water interface. Inset shows electron diffraction. (b) Velocity change of DPA-MOF particle as the hexafluoropropanol is injected at 42s. (c) Velocity change of DPA-MOF particles in different loading amount of DPA from 10% to 30% DPA-to-MOF weight ratios. (d) Design of the MOF boat. A particle in the center of boat shows the location to amount the DPA-MOF particle. (e) An overlaid light microscopic image composed of three images taken every 0.5 second. (f) Comparison of velocity and lifetime of movement between the DPA-MOF particle and the boat incorporating the DPA-MOF particle.